

## THE CLEO ELECTROMAGNETIC CALORIMETER

P. Skubic

Department of Physics and Astronomy  
University of Oklahoma  
Norman, Oklahoma 73019

CLEO is an all purpose magnetic detector presently in operation at the Cornell Electron Storage Ring. The CLEO detector, shown in Fig. 1, has been described in detail elsewhere.<sup>1</sup> The electromagnetic calorimeter will be described here and results from early running of CLEO will be presented.

Detector Design and Construction

The primary electromagnetic detector covers 50% of  $4\pi$  solid angle and is segmented into octants which form a barrel located at a radius of 2 meters from the beam line outside the 0.7 radiation length thick solenoid coil. Each octant is composed of 44 layers of proportional tubes interleaved with 0.2 r.l. thick lead, giving a total thickness of 11.3 r.l. (see Fig. 2). Alternating tube layers were crossed at 90 degrees and were epoxied together two layers at a time, and cured under a compression of 10 tons in order to maintain flatness of the tubes. Each octant forms a rigid, monolithic, self-supporting structure weighing approximately 10 tons. The signal wires from each octant are ganged in 774 groups of from 2 to 20 tubes as shown in Fig. 3. The width of the gangs corresponds roughly to the variation in average shower size with depth. The operating voltage is typically 1520 volts.

The signal grounds are tied to a support box which completely surrounds the detector body. The 0.5  $\mu\text{f}$  capacitance between the box and body provides an

AC ground as well as a convenient way to apply a uniform calibration pulse which is used to correct for variation in amplifier gain.

The input gas composition of 91% argon and 9% methane is trimmed to approximately 2% of the minor component and is constantly monitored by a binary gas analyzer. Bhabha events in the detector are used to eliminate long term drifts and provide an absolute energy calibration.

The solid angle (10% of  $4\pi$ ) near the beam line is covered by two pole tip shower counters as shown in Fig. 1. The mechanical design and construction is similar to that of the primary detector (see Fig. 4). Each module consists of 21 layers of tubes interleaved with 2 mm thick lead, giving a total thickness of 10 r.l.

At the ends of each of the eight dEdx particle identification modules, there are octant end shower counters. These detectors (see Fig. 5) each consist of 16 layers of tubes interleaved with 2 mm lead and cover a combined solid angle of 12% of  $4\pi$ . A summary of the shower counter design parameters is given in Table I.

#### Electron Test Beam Results

The first completed octant was tested in an electron beam at Wilson Synchrotron Laboratory. Shown in Fig. 6 is the response of the detector to normally incident electrons as a function of beam momentum. To determine the rms energy resolution, the data at each energy were fit to a Gaussian function. Figure 7 shows the data from one 0.42 GeV run where the curve is the result of the fit which gave an rms width of  $0.096 \pm 0.003$  with a  $\chi^2$  per degree of freedom of 0.91.  $\sigma/E$  is plotted versus  $1/\sqrt{E}$  in Fig. 8 where the error bars

include statistical and systematic errors. The systematic errors were estimated from the variation in fit parameters for runs taken under similar conditions. The data are reasonably well represented by a straight line with an rms resolution of  $15\%/\sqrt{E}$ .

#### Results from Electron-Positron Data

Figure 9 shows typical  $\mu^+\mu^-$  and  $e^+e^-$  events for electron-positron collisions with a center of mass energy of 10 GeV. Clear minimum ionizing tracks are observed in the shower counter for the  $\mu^+\mu^-$  event indicating good efficiency. Cosmic ray studies indicate that the efficiency for minimum ionizing tracks is greater than 90% for each 2-tube layer. Two back-to-back showers are observed in the  $e^+e^-$  event. The total energy observed in the octant shower counter for  $e^+e^- \rightarrow e^+e^-$  and  $e^+e^- \rightarrow \gamma\gamma$  events is shown in Fig. 10.

The distribution of the sum of azimuthal angles measured for  $\gamma\gamma$  events is shown in Fig. 11. The distribution is centered at 0 as expected with a width of about 9 mrad. The peaks at 104 mrad are due to Bhabha events in which the electron and positron are bent by the magnetic field.

Figure 12 shows the angular distribution of Bhabha events in the octant shower counters where the curve is the expected theoretical distribution. The octant and pole tip counters provide the best measurement of the absolute luminosity for the CLEO detector. The ratio of the luminosity independently measured by the two detectors is plotted in Fig. 13 for a set of runs. Each point corresponds to 20,000 events in the pole tip counter and 1600 events in the octant counter. The average ratio is  $0.976 \pm 0.005$  and is constant within errors.

The octant shower counter has been used to reconstruct  $\pi^0$ 's. In Fig. 14 the  $\gamma-\gamma$  mass distribution is shown separately for photon energies greater than 200 MeV and 600 MeV. In both cases a clear peak is observed at the  $\pi^0$  mass

although the combinatorial background is large for the more numerous lower energy photons.

Electrons with energies above 1 GeV have been identified using the octant shower counter.<sup>2</sup> Using simple cuts on the average number of hits per layer and the ratio of shower chamber energy and momentum measured by the inner drift chamber, a rejection factor of 20 was obtained with an efficiency of ~80% for tracks within the octant counter solid angle. When used in conjunction with the dE/dx chamber, a rejection factor >100 was obtained with an efficiency of 50% for tracks within the fiducial volume.

In summary, the CLEO electromagnetic calorimeter has provided: 1) measurement of photon position and energy over 70% of  $4\pi$  solid angle, 2) electron identification with dE/dx counters, 3) measurement of charged particle positions, 4) a neutral energy trigger, and 5) measurement of storage ring luminosity using Bhabha scattering. The detector has met design goals with stable operation and convenient monitoring.

### Acknowledgments

The octant shower detectors were constructed by our group at Rutgers including: J. J. Mueller, D. Bechis, G. K. Chang, R. Imlay, D. Potter, F. Sannes, P. Skubic, and R. Stone.

The octant end and pole tip detectors were constructed at Harvard by: C. Bebek, J. Haggerty, M. Hempstead, J. M. Izen, R. Kline, W. A. Loomis, W. W. MacKay, F. M. Pipkin, J. Rohlif, W. Tanenbaum, and Richard Wilson.

### References

D. Andrews, et al., The CLEO Detector, Laboratory of Nuclear Studies, CLNS 82/538 (1982).

C. Bebek, et al., Evidence for New-Flavor Production at the  $\gamma$  (4S), Phys. Rev. Lett. 46, 84 (1981).

TABLE I

Shower Counter Parameters

	<u>Octant</u>	<u>Octant End</u>	<u>Pole Tip</u>
<b>Anode Wires</b>			
dia, material	50 $\mu$ gold plated tungsten	25 $\mu$ gold plated tungsten	25 $\mu$ gold plated tungsten
number layers, groups, total	44, 774, 3826	16, 196, 880	21, 711, 2352
alignment	azimuthal and z	azimuthal +22 1/2° -22 1/2° to radial	+120° -120° - to vertical
ganging	12 planes; 2 deep x 1 wide 12 planes; 3 deep x 2 wide 20 planes; 5 deep x 4 wide	4 planes; 1 deep x 2 wide 4 planes; 2 deep x 4 wide 8 planes; 2 deep x 8 wide	6 planes; 1 deep x 1 wide 6 planes; 2 deep x 2 wide 9 planes; 3 deep x 4 wide
<b>Tube size</b>	31.7 mm x 12.7 mm 1.24 mm wall	19 mm x 9.5 mm 1.60 mm wall	19 mm x 9.5 mm 160 mm wall
<b>Lead Sheet (Thickness)</b>	1.27 mm	1.98 mm	1.98 mm
<b>Total</b>	12 r.l.	11 r.l.	10 r.l.
<b>Dimensions</b>	Active length 3.70 m max. active width 2.23 m distance to interaction point 2.36 m to 2.97 m	Active width 1.54 m active height .83 m min. distance to beam line 1.32 m	inside active radius 27.9 cm outside active radius 81.3 cm distance to interaction point 1.19 m to 1.50 m
<b>Solid Angle Coverage</b>			
$\epsilon_{\min}$ , $\epsilon_{\max}$	55°, 125°	40°, 51°	13°, 29°
$\Omega/4\pi$	0.47	0.12	0.10
<b>Gas</b>	91% argon, 9% methane	91% argon, 9% methane	91% argon, 9% methane

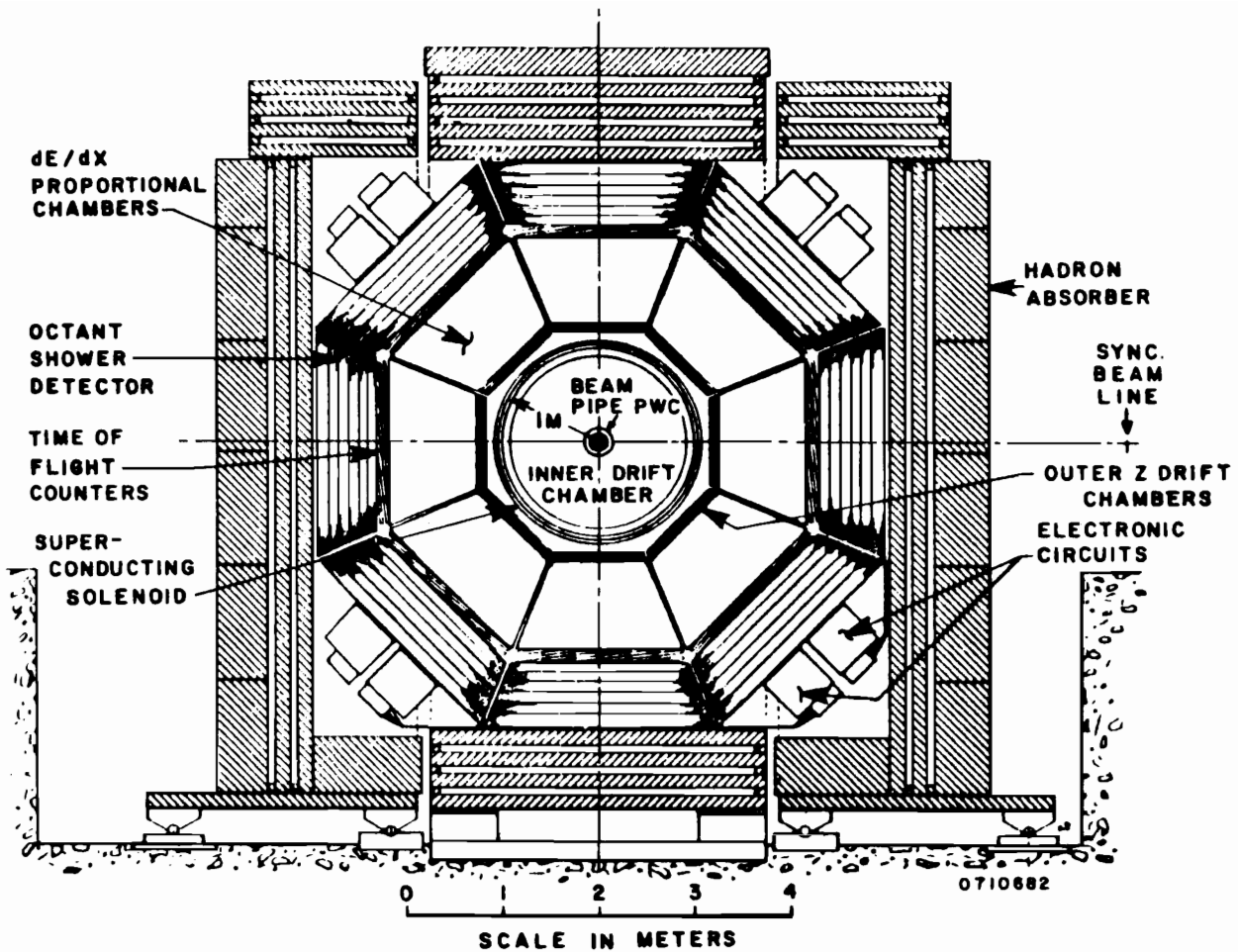


Fig. 1(a)

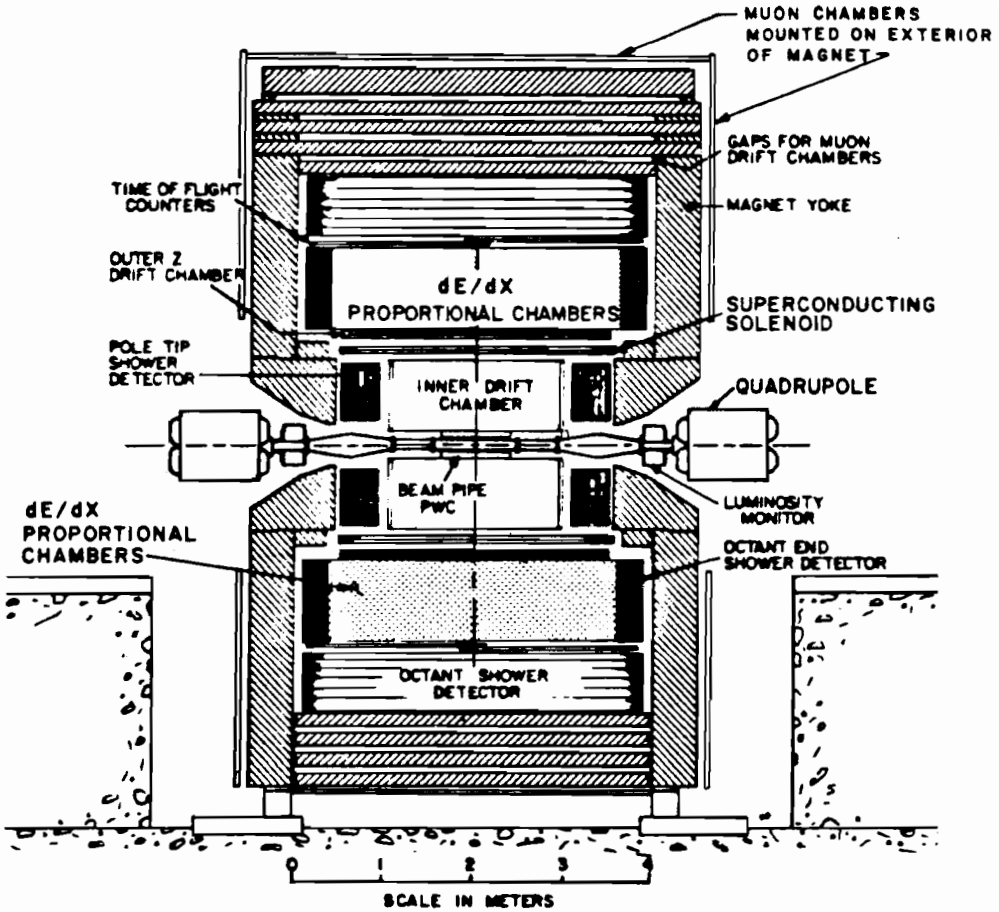


Fig. 1(b)

0710282



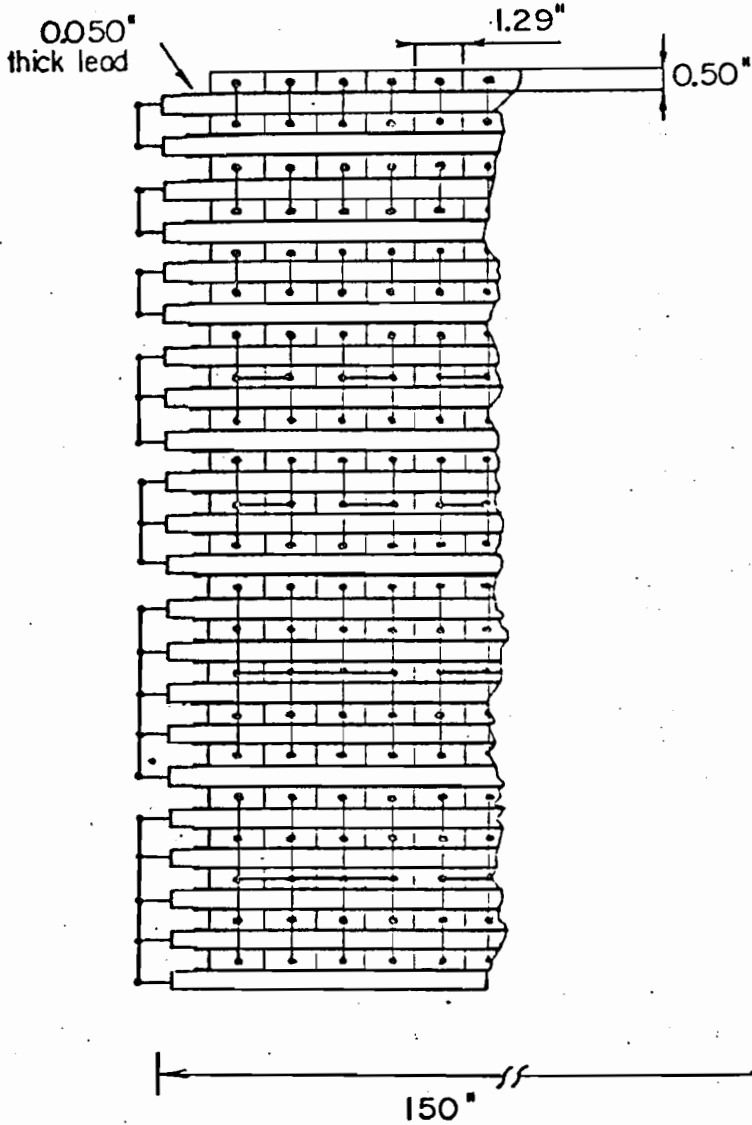
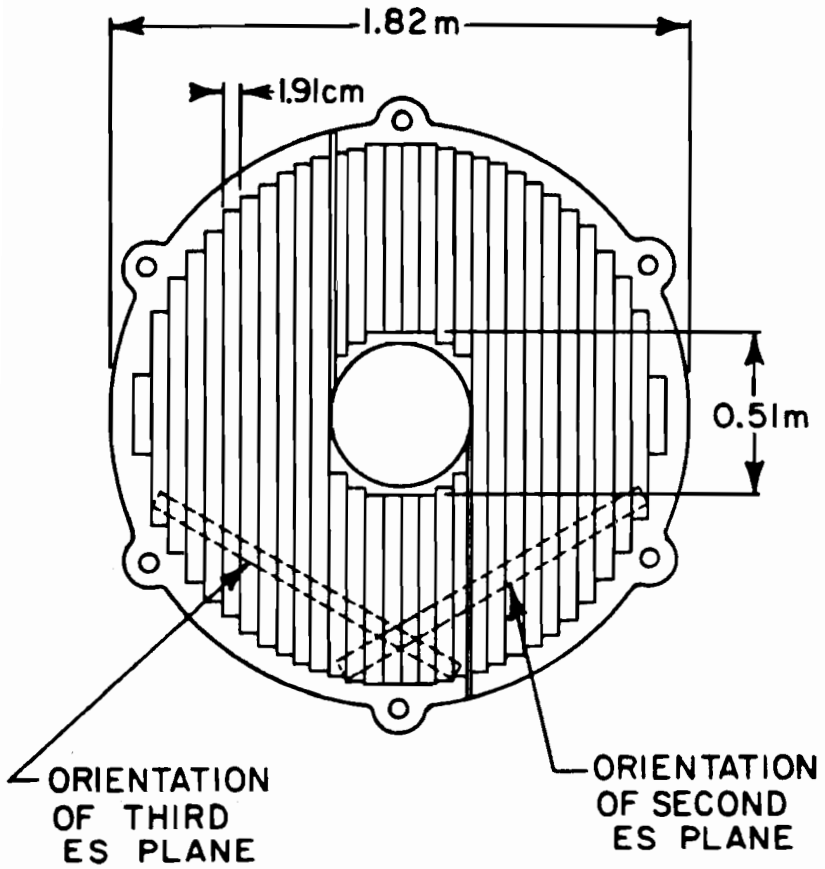


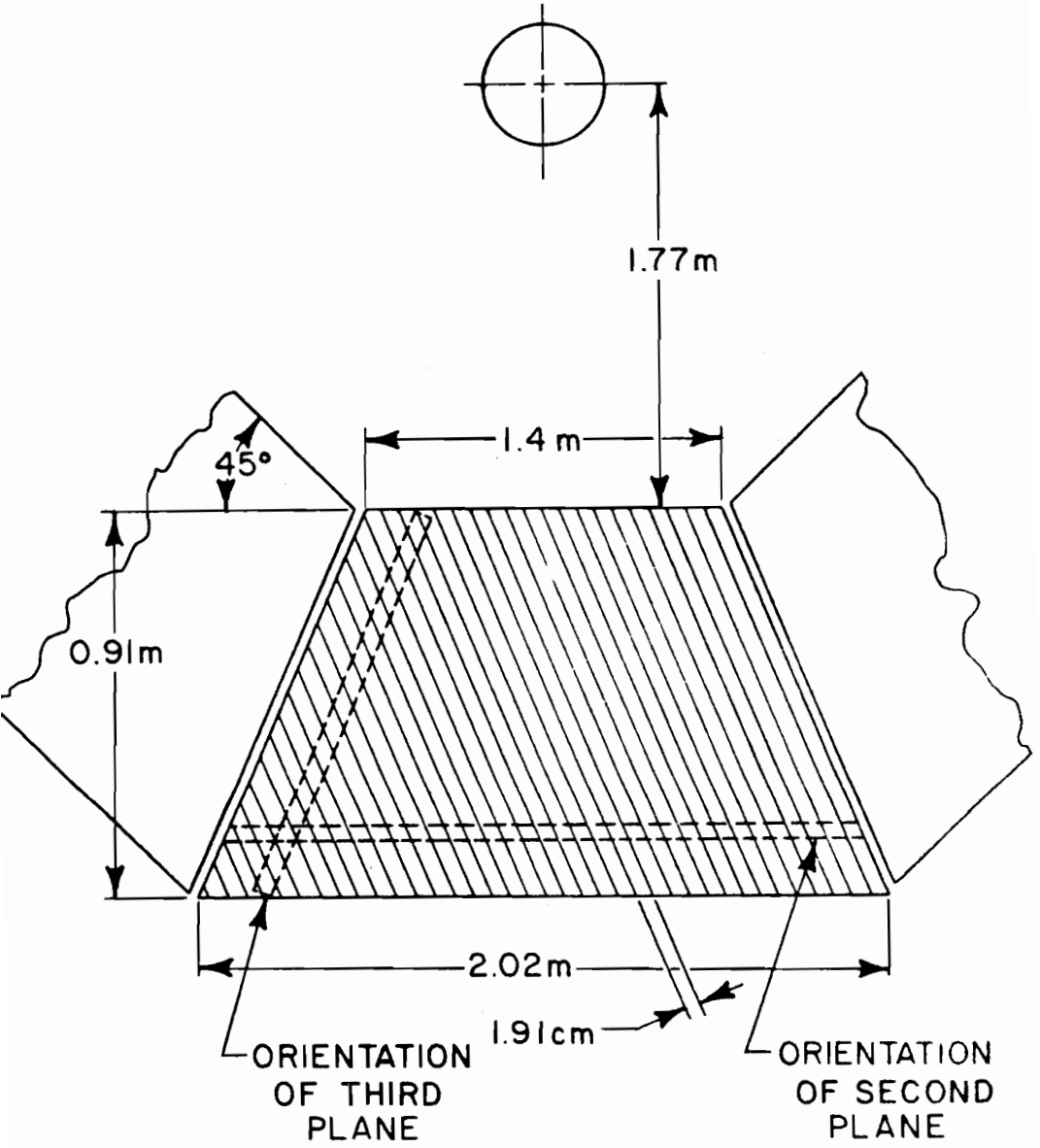
Fig. 3



A SINGLE PLANE OF THE  
POLE SHOWER COUNTERS

Fig. 4

0710382



A SINGLE PLANE OF THE OCTANT END SHOWER COUNTERS.

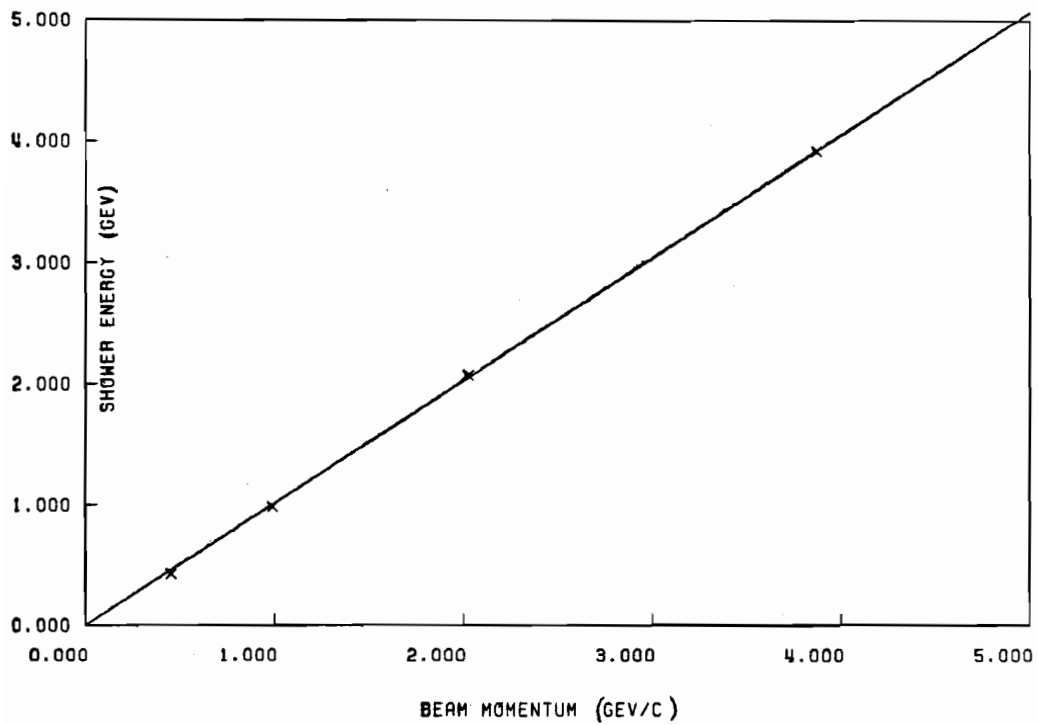


Fig. 6

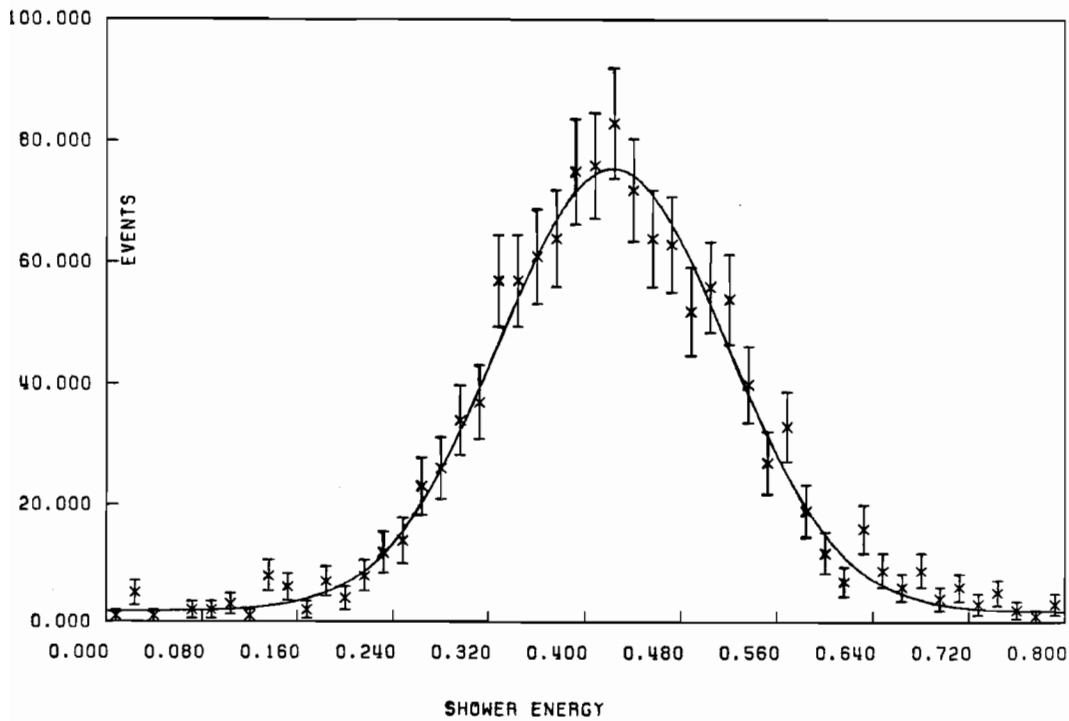


Fig. 7

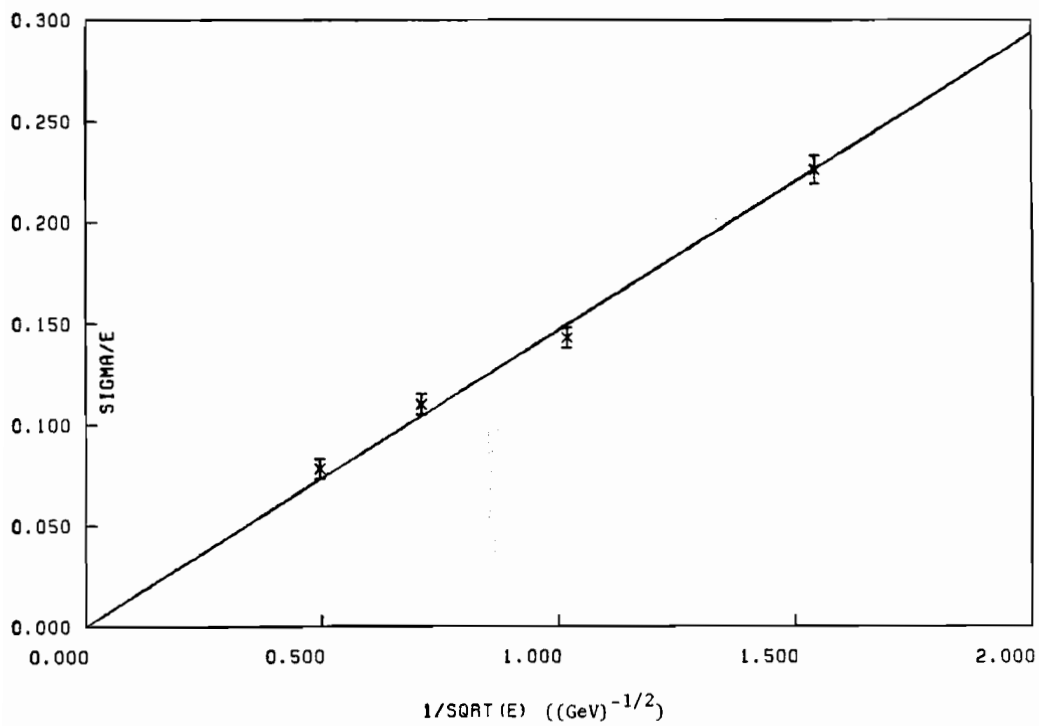


Fig. 8

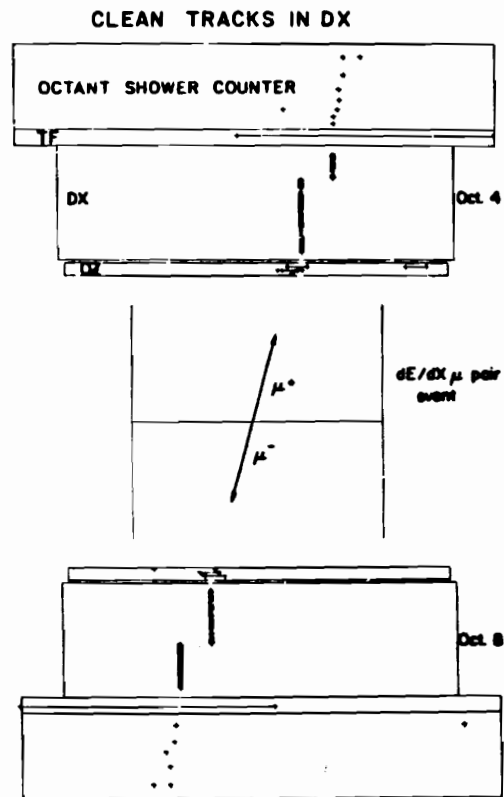
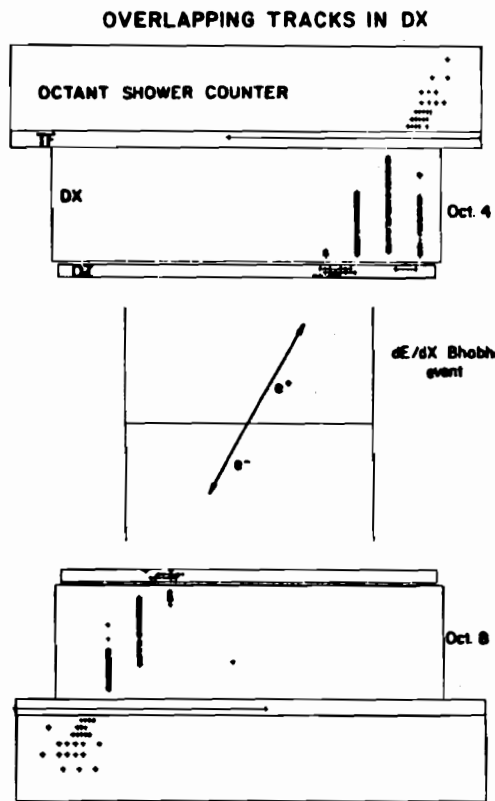
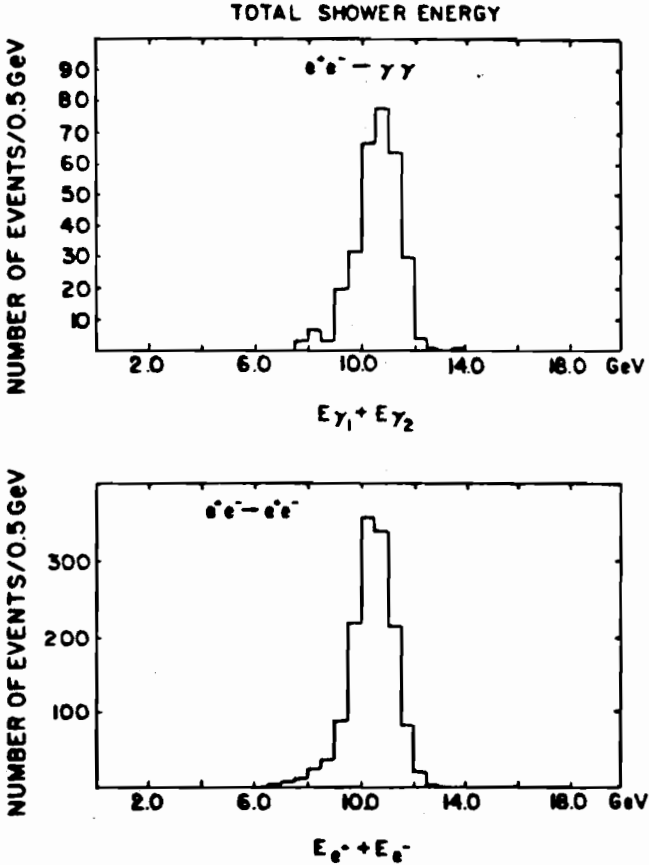


Fig. 9



0710302

Fig. 10

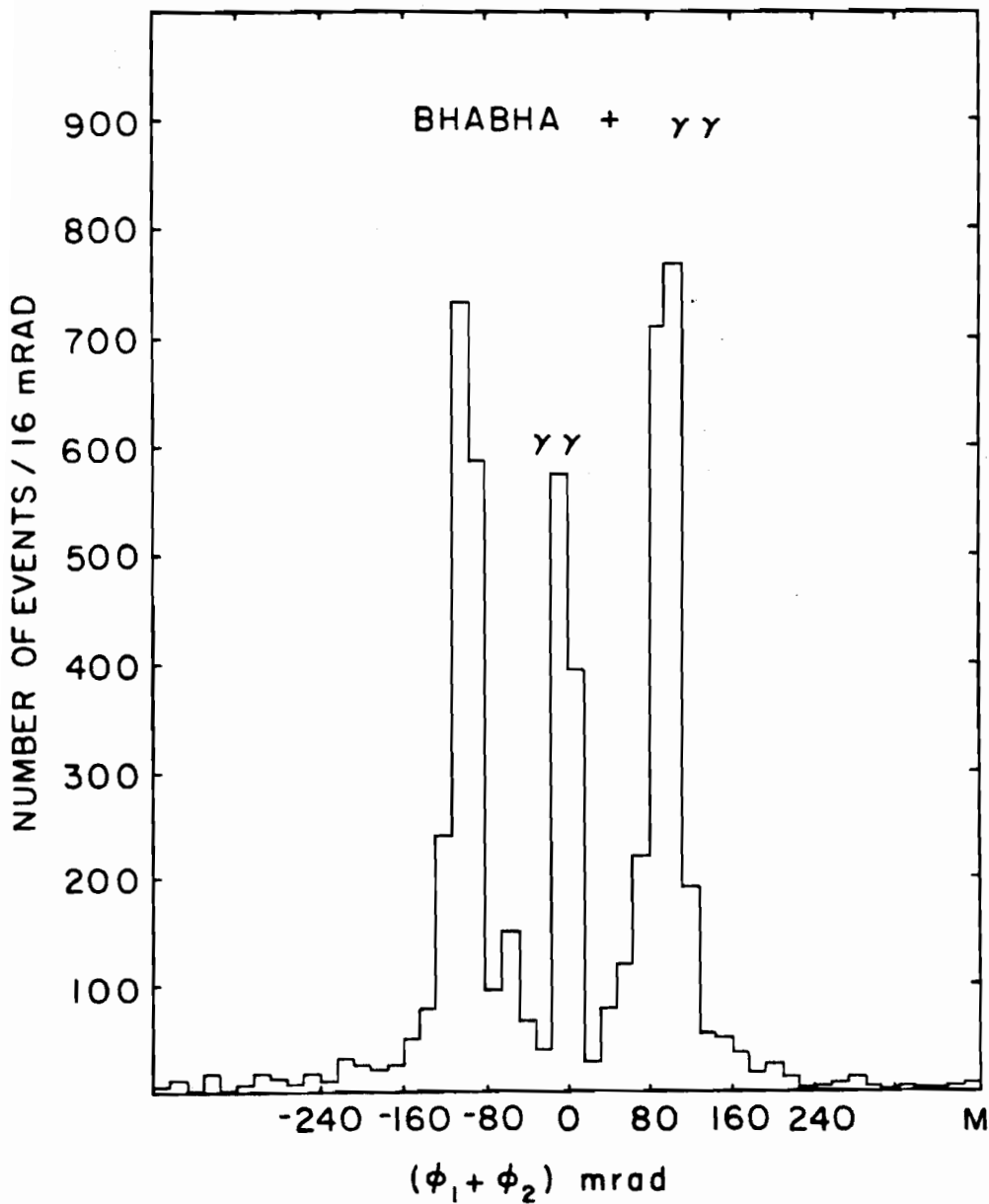


Fig. 11

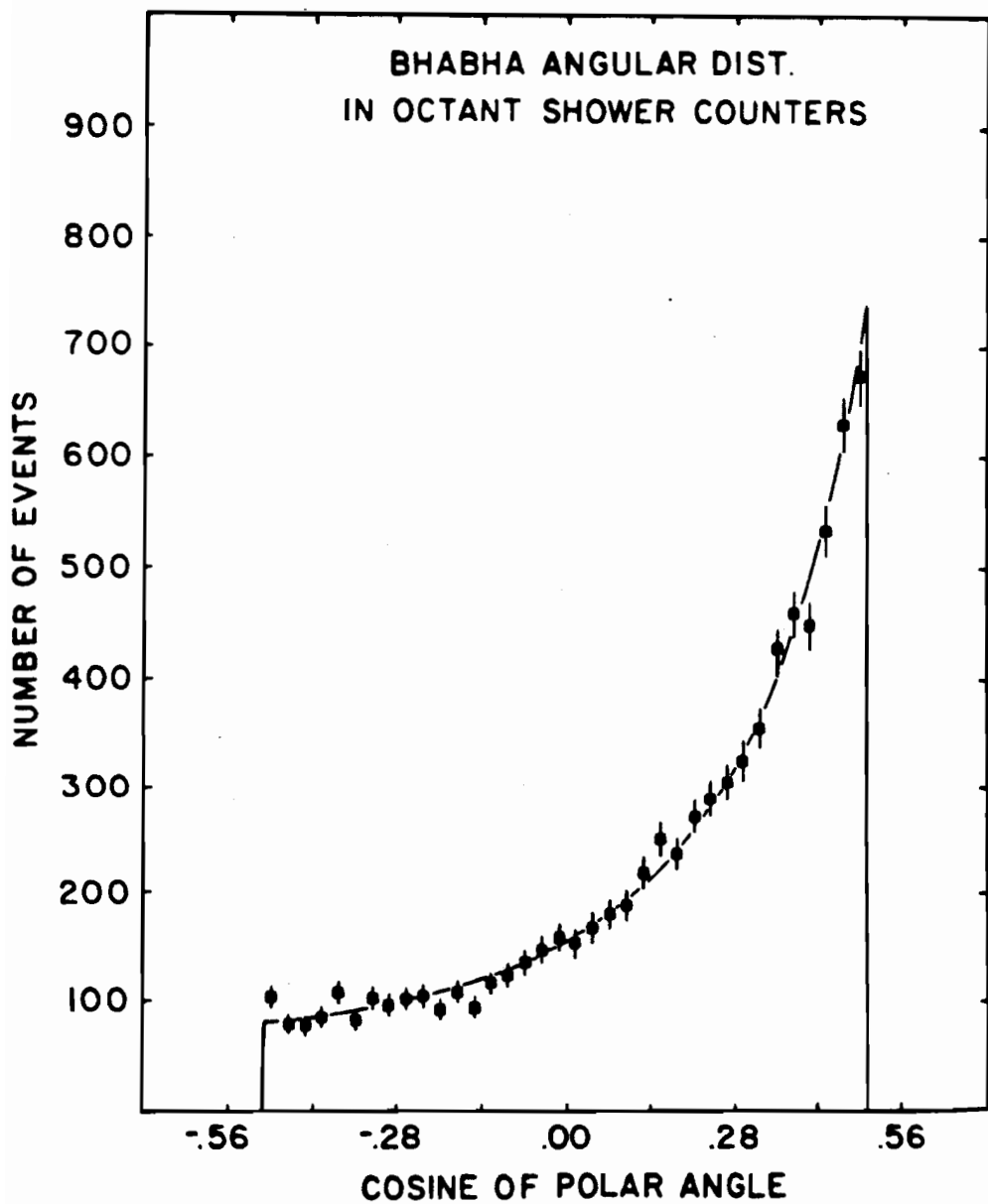


Fig. 12

0710382

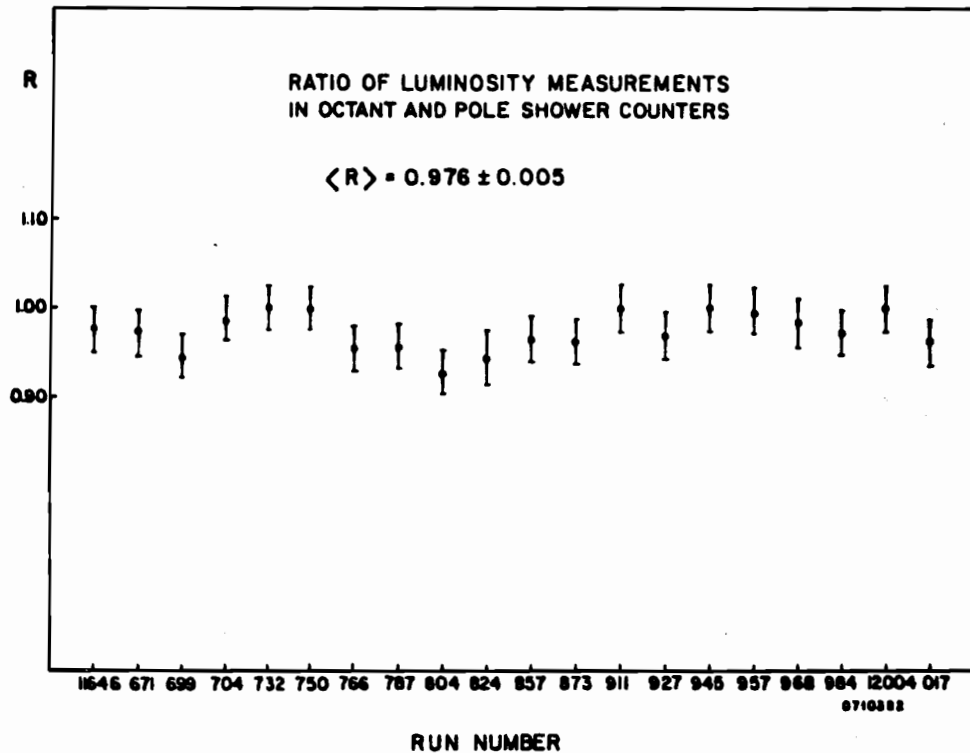


Fig. 13

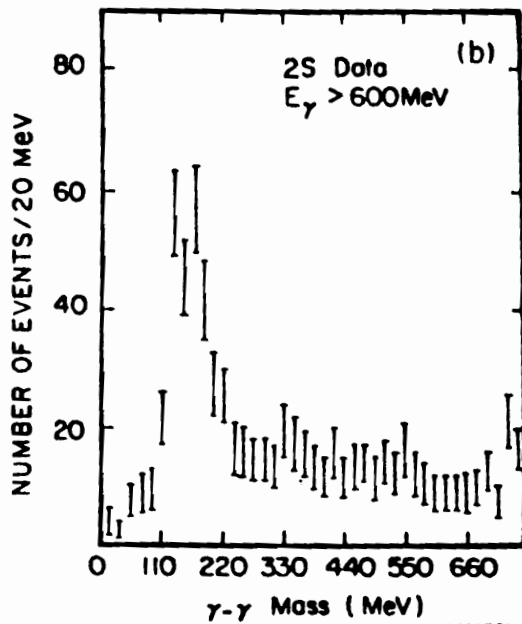
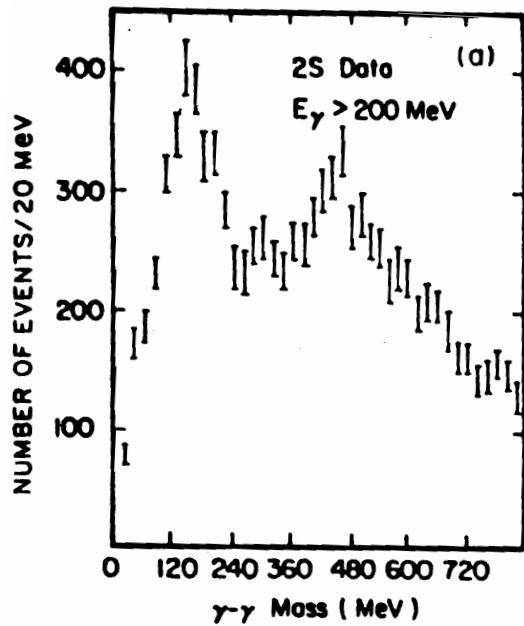


Fig. 14